PeerJ Preprints NOT PEER-REVIEWED

Rapid remote sensing assessment of impacts from Hurricane Maria on forests of Puerto Rico

Yanlei Feng[1], Robinson I. Negron-Juarez[2], Christina M. Patricola[2], William D. Collins[2], Maria Uriarte[3], Jazlynn S. Hall[3], Nicholas Clinton[4], Jeffrey Q. Chambers[*,1,2]

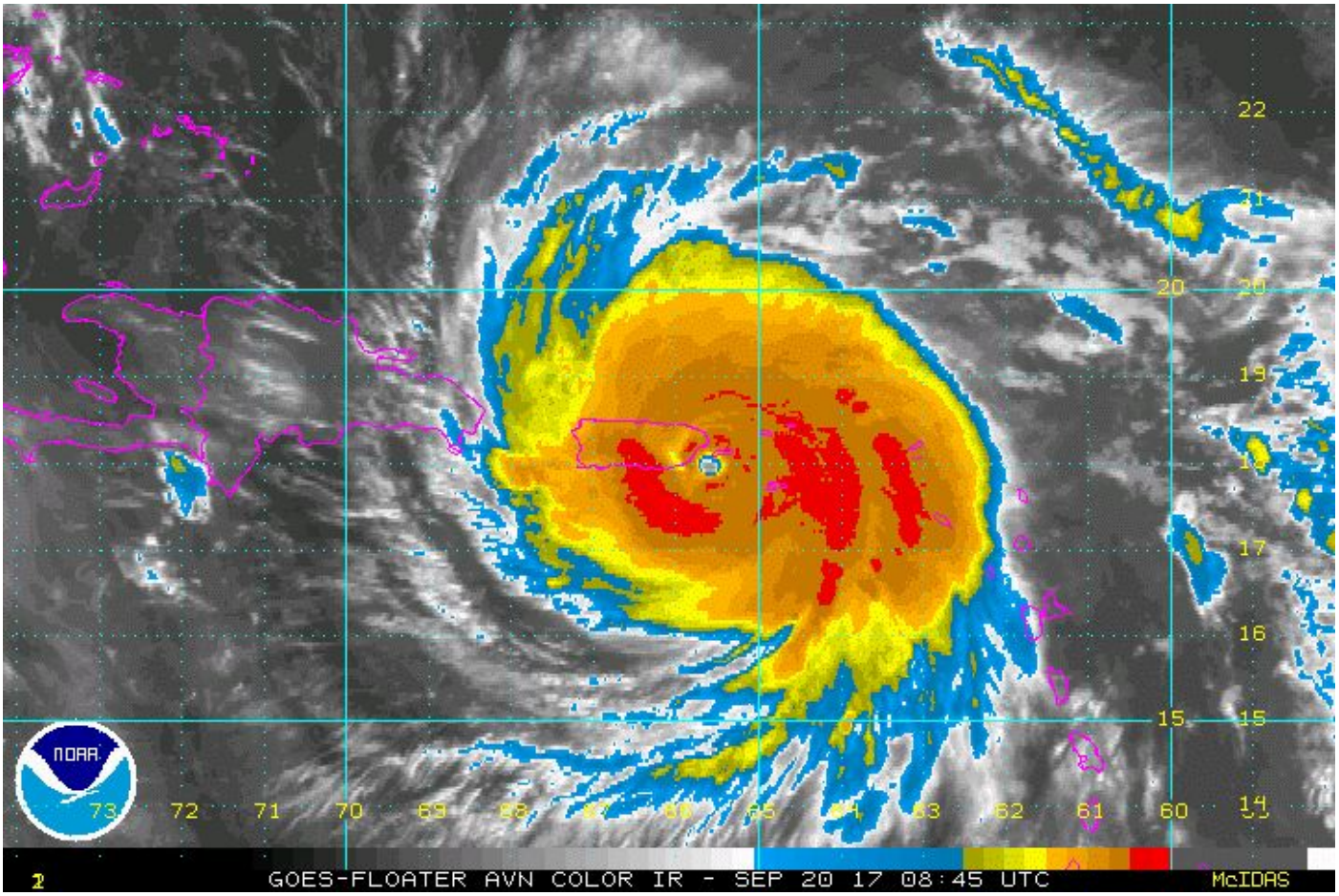

Photo credit: NOAA

[1]*University of California, Department of Geography, Berkeley, California, USA*
[2]*Lawrence Berkeley National Laboratory, Climate and Ecosystem Sciences Division, Berkeley, California, USA*
[3]*Columbia University, Department of Ecology, Evolution & Environmental Biology, New York, New York, USA*
[4]*Google, Mountain View, California, USA*

*corresponding author: jchambers@lbl.gov

PeerJ Preprints | https://doi.org/10.7287/peerj.preprints.26597v1 | CC BY 4.0 Open Access | rec: 1 Mar 2018, publ: 1 Mar 2018

Abstract:
Hurricane Maria made landfall as a strong Category 4 storm in southeast Puerto Rico on September 20th, 2018. The powerful storm traversed the island in a northwesterly direction causing widespread destruction. This study focused on a rapid assessment of Hurricane Maria's impact to Puerto Rico's forests. Calibrated and corrected Landsat 8 image composites for the entire island were generated using Google Earth Engine for a comparable pre-Maria and post-Maria time period that accounted for phenology. Spectral mixture analysis (SMA) using image-derived endmembers was carried out on both composites to calculate the change in the non-photosynthetic vegetation (ΔNPV) spectral response, a metric that quantifies the increased fraction of exposed wood and surface litter associated with tree mortality and crown damage from the storm. Hurricane simulations were also conducted using the Weather Research and Forecasting (WRF) regional climate model to estimate wind speeds associated with forest disturbance. Dramatic changes in forest structure across the entire island were evident from pre- and post-Maria composited Landsat 8 images. A ΔNPV map for only the forested pixels illustrated significant spatial variability in disturbance, with emergent patterns associated with factors such as slope, aspect and elevation. An initial order-of-magnitude impact estimate based on previous work indicated that Hurricane Maria may have caused mortality and severe damage to 23-31 million trees. Additional field work and image analyses are required to further detail the impact of Hurricane Maria to Puerto Rico forests.

Author Comment: The analyses and results from this work represent a rapid response capability following natural disasters impacting forested ecosystems. Datasets are publicly available, and a set of user interface tools is being developed for a variety of stakeholder end uses. These tools and resources will be further developed, and provided on the NGEE-Tropics website (https://ngee-tropics.lbl.gov/hurricane-maria-impacts-to-puerto-rico/)

Introduction

Hurricane Maria made landfall as a strong Category 4 (Saffir-Simpson hurricane wind scale) storm with maximum sustained winds of ~250 km h^{-1} near Yabucoa Harbor in far southeast Puerto Rico early morning of September 20th, 2018 (Fig. 1). Maria traversed Puerto Rico in a northwest direction, exiting near the city of Arecibo, and causing widespread destruction across the island. A few weeks earlier on September 6th, Category 5 Hurricane Irma had passed within ~80 km north of the island, with sustained winds of ~300 km h^{-1}, and damage primarily in the northwest region of the island. This report is focused on the impacts of these powerful storms on Puerto Rico's forests, with an emphasis on the impacts of Hurricane Maria.

Cyclonic storms represent a dominant natural disturbance in temperate and tropical forests in coastal regions of North and Central America (Boose *et al*. 1994, Everham and Brokaw 1996, Mabry, *et al*. 1998, Platt *et al*. 2000, McNab *et al*. 2004). Given Puerto Rico's location in the northeast Caribbean between the Caribbean Sea and Atlantic Ocean, the island is vulnerable to hurricane impacts. In the second half of the 20th century, the island was struck by two severe hurricanes and several minor storms. After a 66-year period with relatively little hurricane damage, Hurricane Hugo, a Category 4 storm, struck the island in September 1989 causing

PeerJ Preprints | https://doi.org/10.7287/peerj.preprints.26597v1 | CC BY 4.0 Open Access | rec: 1 Mar 2018, publ: 1 Mar 2018

significant damage (see summary of effects in Tanner *et al.* 1991). As forests were recovering from Hurricane Hugo, Hurricane Georges struck Puerto Rico in September 1998 with winds up to 150 km h^{-1} (Category 3, Miner Solá 2000). Based on records extending back into the late 1800s, Hurricane Maria was the second most powerful storm to hit the island, surpassed only by the 1928 San Felipe Segundo hurricane. Other recent landfalling Puerto Rico hurricanes include Georges 1998 (Category 2), Hortense 1996 (Category 1), Hugo 1989 (Category 3), and San Ciprian 1932 (Category 2). Hurricane Georges followed a path similar to Maria after landfall, but then exited on the far southwest of the island (Fig. 1).

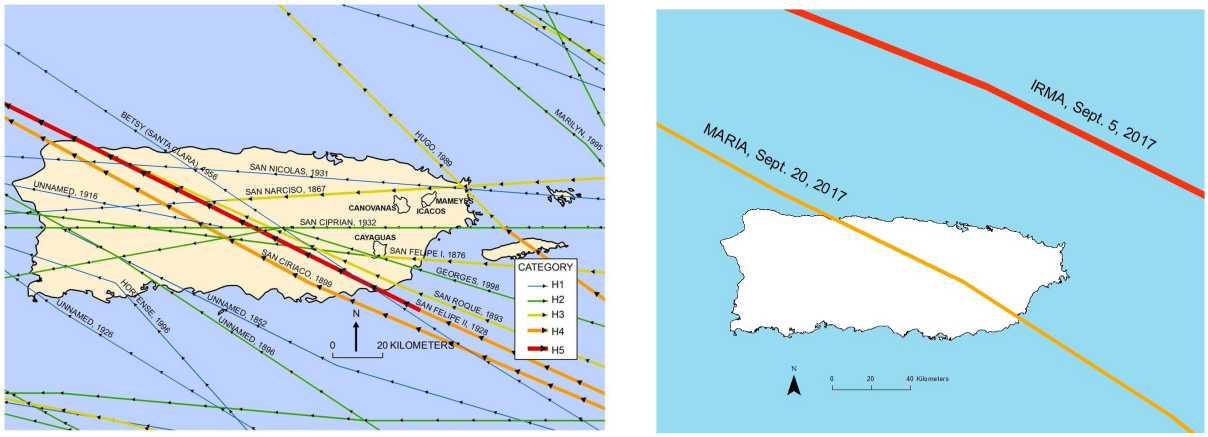

Figure 1 - A sample of historical hurricanes that have struck Puerto Rico (USGS, public domain https://www.usgs.gov/media/images/puerto-rico-hurricanes-map) and tracks for hurricanes Maria and Irma

Hurricanes Hugo and Georges stimulated a large amount of research on the effects of wind disturbance on tropical forests (e.g. Tanner et al. 1991, Yih *et al*. 1991, Bellingham 1991). Generally, tall forests with denser canopies are more susceptible to wind damage (Everham and Brokaw 1996), suggesting increased vulnerability of older forest stands (Flynn *et al.* 2010). On the other hand, a dense, well-developed canopy may reduce tree mortality from tip-ups in water-logged soil (Arriaga 2000, Lugo 2008). Tree species differ strikingly in their susceptibility to hurricane disturbance (Zimmerman *et al.* 1994, Canham et al. 2010) and the nature of their recovery from wind disturbance (e.g. Walker 1991, Zimmerman *et al.* 1994, Uriarte et al. 2009, Canham et al. 2010). In general, pioneer and secondary forest species are more susceptible to damage than shade tolerant species, suggesting that second-growth forests dominated by these species may be more vulnerable to wind damage.

A few studies examined the impacts of hurricanes at the landscape scale (Boose et al. 1994, Foster et al. 1999, Flynn et al. 2010). These studies suggest that forests growing at high elevation or on windward slopes are more exposed to wind damage, and may experience greater mortality from storm events (Everham & Brokaw 1996, Arriaga 2000, Bellingham & Tanner 2000, Boose *et al*. 2004). The observed associations between topography and tree damage may also be mediated by soil characteristics. Trees growing in shallow soils on ridges

PeerJ Preprints | https://doi.org/10.7287/peerj.preprints.26597v1 | CC BY 4.0 Open Access | rec: 1 Mar 2018, publ: 1 Mar 2018

or hilltops, on steeper slopes, or on soils with poor drainage have more restricted root growth, and as a result may be more vulnerable to wind-throw and stem break (Everham & Brokaw 1996, Arriaga 2000, Bellingham & Tanner 2000). When controlling for exposure to winds, hurricane disturbance also exerted stronger effects on older forests, with greater damage and basal area losses for large trees and less damage in younger stands (Foster et al. 1999, Flynn et al. 2010).

More recently, satellite remote sensing approaches have enabled the spatially explicit mapping of disturbance impacts on forested ecosystems, providing additional insights into the ecological effects of these storms (Frolking et al. 2009, Chambers et al. 2007). For Puerto Rico, Ayala-Silva and Twumasi (2004) demonstrated a significant relationships between distance from the hurricane track and changes in the normalized difference vegetation index (NDVI) using data from the Advanced Very High Resolution Radiometer (AVHRR-14). Rainfall induced landslides in Puerto Rico are a common natural disaster on the island, and remote sensing approaches are also valuable for assessing these mudflow hazards (Hong et al. 2006).

Remote sensing approaches have also been employed to quantify the impacts of hurricanes on forests in other regions. Chambers et al. (2007) employed a method linking extensive field-based tree mortality surveys with spectral mixture analysis (SMA) on Landsat and MODIS imagery to quantify the impact of Hurricane Katrina on U.S. Gulf Coast forests at scales ranging from <1000 m^2 to the entire impacted region, providing an estimate of the total number of trees dead or damaged by the storm. Negron-Juarez et al. (2010) and Negron-Juarez et al. (2014) extended this work to include the forest impacts from hurricanes Rita, Gustav, and Charlie, and tropical cyclone Yasi that made landfall in the forested region of northeastern Australia.

Variable wind speeds from landfalling tropical cyclones can drive strong spatial patterning in forest tree mortality and damage impacts. Wind speeds generally decrease as the storm moves onshore, and are also modified by elevation, slope, and aspect. Boose et al. (1994) developed a simple model that combines information on the track and intensity of a hurricane. The model assumes that movement over land decreases sustained wind speeds, increases inflow angles and topographic heterogeneity to calculate spatial variation in sustained damage. This model accurately reconstructed historical exposure to hurricane winds in Puerto Rico at the landscape scale, when compared to historical records (Boose *et al.* 1994, 2004, Foster *et al.* 1999). Previous work has also demonstrated significant correlations between wind speed estimates using models (e.g. H*wind, Powell et al. 1998), and forest damage determined by spectral shifts before and after the storm (Chambers et al. 2007, Zeng et al. 2009, Negron-Juarez et al. 2014, Rifai et al. 2016, Schwartz et al. 2017).

An important aspect of developing an improved understanding of mechanisms controlling spatial variability of tropical cyclones impacts on forested ecosystems is the availability of high-resolution wind velocity maps. Wind maps enable quantification of critical force thresholds in the snapping and uprooting of trees, and in determining the effects of slope and topographic position. Improving our understanding of treefall thresholds are also important for improved

PeerJ Preprints | https://doi.org/10.7287/peerj.preprints.26597v1 | CC BY 4.0 Open Access | rec: 1 Mar 2018, publ: 1 Mar 2018

hazard assessments, with falling trees, for example, being a major source of impact to power lines. Ideally, wind velocity information would be derived entirely from observations. However, station data are available only at a few points, and it is challenging to derive terrestrial winds from satellite data. Climate model simulations at convection-permitting resolution can supplement observations to provide the high-resolution maps of wind velocity suitable for understanding tropical cyclone impacts on forests.

Methods

Study area

The island of Puerto Rico is a United States territory located in the Caribbean, centered at 18.2°N, 66.4°W and covering an area of about 9000 km^2. The central part of the island is characterized by mountains (40% of the island), surrounded by foothills (35%) and narrow coastal plains (25%), with land-use activities focused on the coastal plains (Miller and Lugo 2009). The Cordillera Central range divides the island north-south and creates climatically distinct regions. Temperature fluctuates little throughout the year with mean minimum in the mountainous areas of 22°C and mean maximum in the coastal areas of 27°C (Gomez-Gomez et al. 2014). The Cordillera Central produces a pronounced orographic effect, intercepting the easterly trade winds and resulting in high rainfall amounts on the windward (north) slopes and plains, while the leeward (south) side of the mountains and plains lie within a rain shadow (Gomez-Gomez et al. 2014). The wet season runs from May to October. The northern coast receives about ~1500 mm per year, the south coast ~900 mm, and mountains receive between 3000 and 4000 mm annually (Gomez-Gomez et al. 2014). Forests cover about 54% of Puerto Rico accounting for 27 million tons of carbon (above and below ground)(Brandeis and Turner 2009). Hurricanes are the primary non-anthropogenic ecological disturbance on the island (Miller and Lugo 2009).

Image Processing

Topographic corrections as well as radiometric inter-calibrations were carried out for Landsat 8 images using Google Earth Engine (GEE) (Gorelick et al. 2017). GEE is a cloud-based platform that includes vast remote-sensing (and other) datasets with associated analysis tools accessed using a JavaScript API, enabling high-performance, intrinsically parallel remote sensing analyses. Landsat 8 raw images collected from June 1st to September 30th in 2016 (pre-disturbance) and from October 1st to October 30th in 2017 (post-disturbance), with less than 40 percent cloud cover, were readily selected as image collections through the platform. The image periods were selected to minimize bias associated with seasonal phenology. The period of maximum greenness in Puerto Rico is from June to October (Fig. 3).

Landsat 8 Level-1 Precision Terrain (L1PT) processed images have well-characterized radiometry, and they have been consistently geo-registered and inter-calibrated across different Landsat sensors. We applied cloud and shadow masks with a one-pixel buffer to the images. The masks were created using Data quality assessment (BQA) band in Landsat 8 with the modified kernel function in GEE. After removing to the extent possible effects of clouds and shadow, the image collections were composited into two (pre-hurricane and post-hurricane) images by selecting only the least-cloudy pixels over this time period. They were also converted

PeerJ Preprints | https://doi.org/10.7287/peerj.preprints.26597v1 | CC BY 4.0 Open Access | rec: 1 Mar 2018, publ: 1 Mar 2018

to top-of-atmosphere reflectance from original encoded radiance values. Post-hurricane images were radiometrically calibrated band by band (Negron-Juarez et al. 2010) with respect to Pre-hurricane images using invariant targets (Furby and Campbell 2001), including 7 features in urban areas, 3 in forests, 4 in lakes, and 1 in farmland. The features were validated against available high-resolution imagery. Then we used Bin et al.'s (2013) illumination correction algorithm to minimize the variability of reflectance caused by topography and bidirectional reflectance distribution effects.

Spectral Mixture Analysis

Snapped and uprooted trees, and trees canopies stripped of leaves, cause a shift in surface reflectance from green vegetation (GV) spectra to non-photosynthetic vegetation (NPV -- exposed wood and surface litter) spectra, a shift dominated by increased reflectance in the shortwave infrared wavelengths (Landsat 8 bands 6 and 7). Forests that experience limited impacts will demonstrate little change in NPV (once surviving trees flush out), and will maintain high GV spectral reflectance. For trees that are only stripped of leaves but survive, this change in the NPV spectral response from before to after the storm (ΔNPV) rapidly shifts back to GV as tree crowns flush with new leaves. A high ΔNPV signal will persist for about a year in tropical forest regions impacted by snapped and uprooted trees. Overall, ΔNPV provides a quantitative measures of the changes in dead vegetation and woody biomass associated with hurricane disturbance (Chambers et al. 2007, Negrón-Juárez et al. 2011).

For this work, we applied SMA (Adams et al. 1995; Shimabukuro and Smith 1991) to the Landsat 8 scenes (bands 2, 3, 4, 5, 6, and 7) to quantify forest disturbance produced by Maria. SMA quantifies the fraction of each endmember that sum to match the full spectrum of each image pixel (Adams et al. 1995). Image-derived endmembers of GV, NPV, and shade were used. The fractions of GV and NPV were normalized without shade as GV/(GV+NPV) and NPV/(GV+NPV) (Adams and Gillespie 2006). This processing was done in GEE.

Fig 2a -- Pre-Maria Landsat 8 false-color image with display colors red as band 6 (SWIR), green as band 5 (NIR), and blue as band 4 (red).

PeerJ Preprints | https://doi.org/10.7287/peerj.preprints.26597v1 | CC BY 4.0 Open Access | rec: 1 Mar 2018, publ: 1 Mar 2018

Fig 2b -- Post-Maria Landsat 8 false-color image with display colors red as band 6 (SWIR), green as band 5 (NIR), and blue as band 4 (red). Heavily impacted areas show up as large increases in SWIR reflectance (red), with some areas also exhibiting a green-up associated with increased NIR reflectance (green).

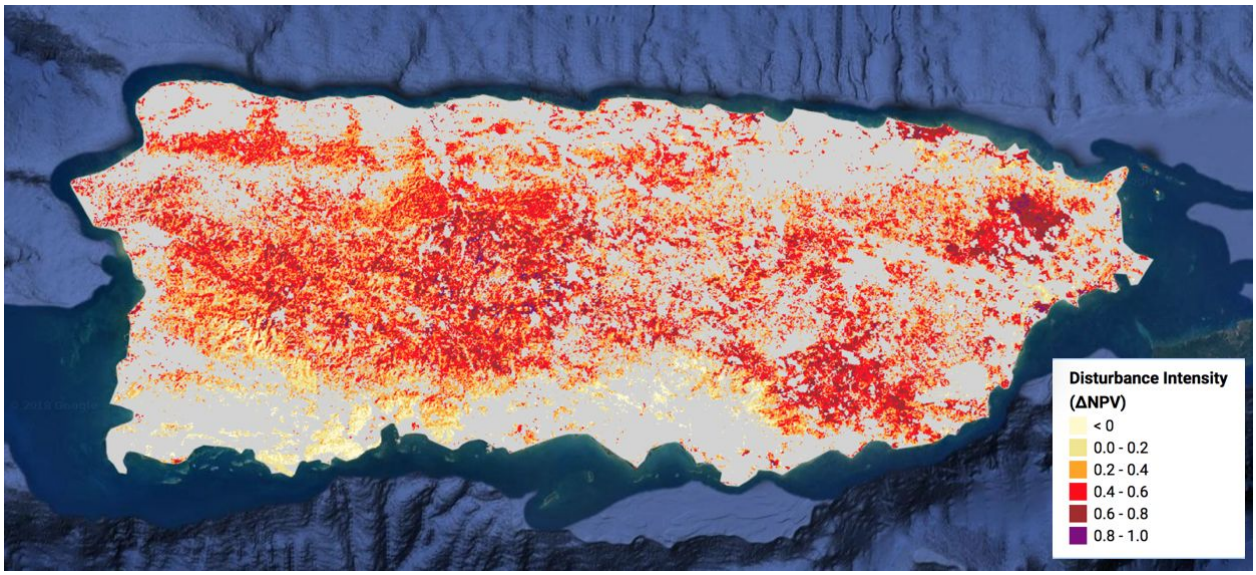

Fig 2c -- ΔNPV map of Puerto Rico forested pixels with highest forest damage and tree mortality impact areas in with darker tones of red indicating more intense forest disturbance as tree mortality and crown damage. Grey areas represent non-forested areas or areas with cloud cover. Datasets for all images available here: http://dx.doi.org/10.15486/ngt/1419953

Time series of EVI

The Enhanced Vegetation Index (EVI) is a vegetation index that enhance the vegetation signal in areas with high biomass and expressed as EVI=G*(NIR-RED)/(NIR+ a*RED-b*BLUE+L) where NIR, RED and BLUE surface reflectance from Moderate Resolution Imaging Spectroradiometer (MODIS) (Justice et al. 1998). Further details are found in Huete et al. (2002).

PeerJ Preprints | https://doi.org/10.7287/peerj.preprints.26597v1 | CC BY 4.0 Open Access | rec: 1 Mar 2018, publ: 1 Mar 2018

EVI has been shown to be appropriate for tropical forest applications (e.g. Huete et al. 2002, Huete et al. 2006). Time series of EVI over Puerto Rico was produced to determine the temporal severity of disturbance caused by hurricane Maria compared to other events over period with MODIS data. Time series of EVI from 2000 to 2017 was produced using the 16 EVI MODIS Terra (data available in GEE).

Forested area mask

To determine forested areas, we used the Hansen Global Forest Change map (version 1.4, 30 m spatial resolution) (Hansen et al. 2013, available in GEE) for 2000, defined as canopy closure including all vegetation taller than 5 m. The data is encoded as a percentage of tree canopy per pixel in the range of 0 - 100, with 50 used as the threshold to define a pixel as a forested pixel. Over Puerto Rico, Evergreen Broadleaf Forest and Deciduous Broadleaf Forest are the dominant forest types in this dataset. A mask containing all forested pixels was applied over the ΔNPV image and time series of EVI.

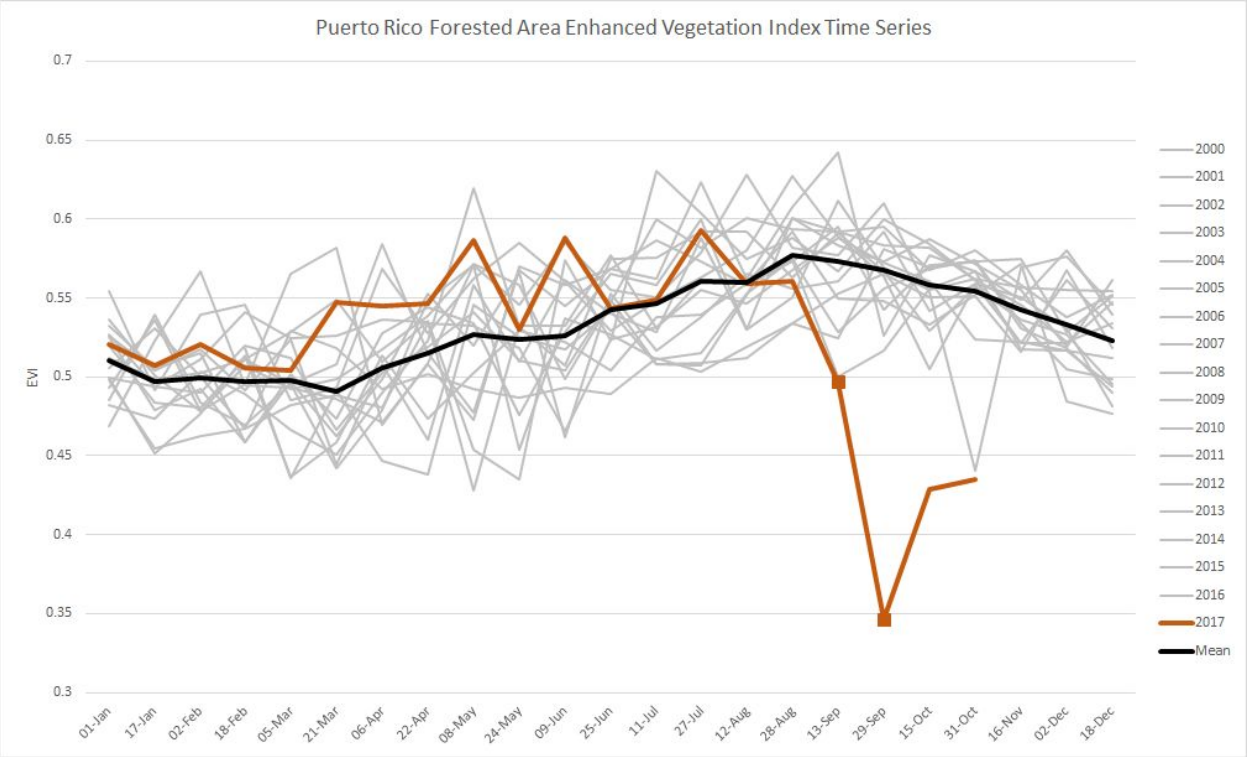

Fig 3 -- Average time series of MODIS EVI from forested pixels across Puerto Rico over 2000-2017 showing the maximum spectral shift immediately following Maria's landfall, and subsequent partial recovery as surviving trees flush out new leaves.

Hurricane Simulations

We performed convection-permitting hindcast simulations of Hurricane Maria with the Weather Research and Forecasting (WRF) regional climate model (Skamarock and Klemp, 2008), which is developed by the National Center for Atmospheric Research (NCAR). The simulations were configured with a horizontal resolution of 4.5 km and 44 levels in the vertical. Initial and lateral

PeerJ Preprints | https://doi.org/10.7287/peerj.preprints.26597v1 | CC BY 4.0 Open Access | rec: 1 Mar 2018, publ: 1 Mar 2018

boundary conditions and sea-surface temperature were prescribed from the 6-hourly, 0.5 National Centers for Environmental Prediction (NCEP) Climate Forecast System version 2 (CFSv2) (Saha et al., 2014). We generated a 10-member ensemble of hindcasts using the Stochastic Kinetic Energy Backscatter Scheme (SKEBS) (Shutts, 2005), with simulations initialized on 00z September 17, 2017 and run through 00z September 25. The hindcasts reproduce the observed peak intensity of Maria reasonably well, with an observed and simulated ensemble-mean maximum 10-m wind speed of 277 km $h^{-1}$and 244 km h^{-1}, respectively. A snapshot of simulated 10-m wind speed prior to Maria's landfall is shown in Fig. 4a. At a horizontal resolution of 4.5 km, the hurricane's eye is apparent, as well as a reduction in wind speed over land relative to ocean. In addition, the model produces a hurricane-total precipitation maximum that generally corresponds to the topography of Puerto Rico (Fig. 4b). Convection-permitting simulations of tropical cyclone events allow us to quantify the impact of anthropogenic climate change, so far and into the future, on tropical cyclone intensity and precipitation, by perturbing model boundary conditions and greenhouse gas concentrations to account for mean climate change (Patricola et al., 2018; Patricola and Wehner, 2018).

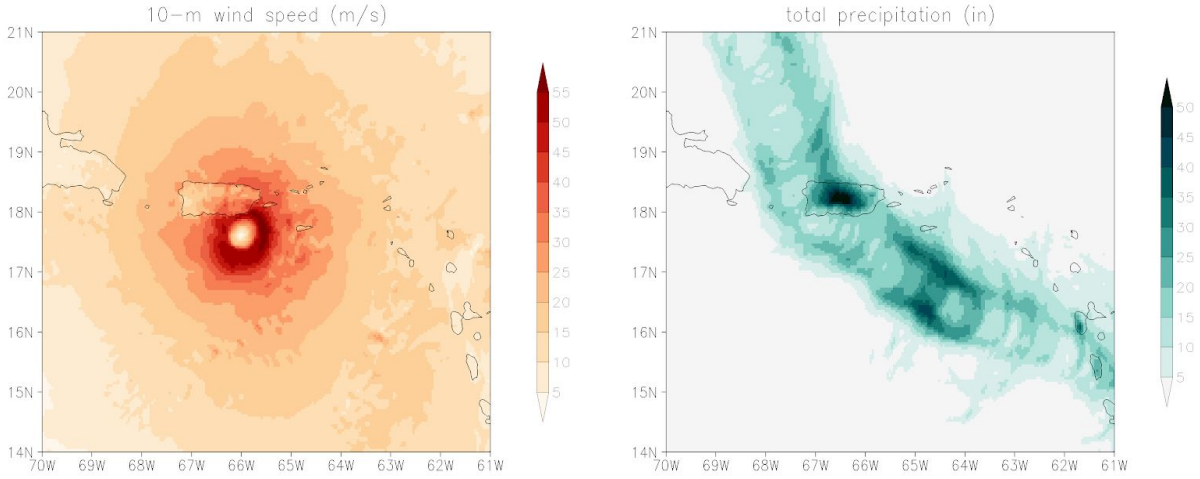

Figure 4. (a) Instantaneous 10-m wind speed (m s^{-1}) and (b) storm-total precipitation (in) from a 4.5 km resolution hindcast simulation of Hurricane Maria.

User Interface tools

We also used Google Earth Engine packages to build a client-side user interface (UI). The UI currently includes a drop down menu, a slider, and legends. In this package, the user can choose an image including pre-hurricane, post-hurricane, and tree disturbance intensity images to visualize. The slider can help user set the opacity of the visualized image, and to toggle between the road and the satellite base map. A simplified version of this UI is available at our project website (https://ngee-tropics.lbl.gov/hurricane-maria-impacts-to-puerto-rico/), which will be updated as the UI tools become available for public versions of our script.

PeerJ Preprints | https://doi.org/10.7287/peerj.preprints.26597v1 | CC BY 4.0 Open Access | rec: 1 Mar 2018, publ: 1 Mar 2018

Results

Pre- and post-Hurricane Maria false-color images clearly illustrate the widespread impact of Hurricane Maria on the island of Puerto Rico as a shift from green to red (Fig. 2a and 2b, respectively). Forested areas that experienced extensive tree mortality and crown damage show up in these images as a decrease in near-infrared (NIR) reflectance associated with the loss of green leaf canopy cover, and an increase in short-wave infrared (SWIR) associated with an increase in reflectance from woody materials and surface litter exposed with the loss of canopy cover. After removing effects of clouds and cloud shadows, carrying out imaging processing and SMA described above, and masking all non-forest pixels, a colorized ΔNPV map was produced (Fig. 2c). This map shows areas with high ΔNPV in red brightness colors (purple-brown-red) indicating high levels of mortality and tree structural damage in ΔNPV.

To quantify some temporal effects of Hurricane Maria on the forests of Puerto Rico, an analysis of the MODIS-EVI vegetation index demonstrated a steep and rapid decline in vegetation greenness (orange line Fig. 3) in comparison to the average and the full range of EVI response since 2000. It appears that the impact of Hurricane Irma on Puerto Rico (with the closest pass north of the island on September 8th) is also evident as a decline in EVI to just outside of the historical range in EVI on from the September 13th, with a much steeper decline in EVI in the subsequent interval out to September 29th associated with the Maria's landfall and crossing of the island on the 20th of September.

As seen in significant variation in the ΔNPV disturbance signal across the island, there are a number of factors driving variable forest impacts from Hurricane Maria. Toward improving our understanding of these factors, we carried out model simulations of predicted wind speed and storm-total precipitation across the island. This simulation data in conjunction with data that will be collected in field campaigns in 2018 will help enable a more mechanistic understanding of factors that control variability in forest vulnerability to hurricane impacts.

Discussion

Previous studies have shown that an increase in NPV from one image to the next (i.e. positive ΔNPV) is positively and linearly correlated with tree mortality and extensive crown damage. This strong relationship between the shift in spectral reflectance and the tree mortality and damage rate has enabled quantitative measures of total tree mortality from storm disturbances. A similar analysis to that carried out here estimated total tree mortality and severe structural damage from Hurricane Katrina of more than 300 million trees (Chambers et al. 2007). This approach has been expanded to other landfalling hurricanes in the U.S. (Negron-Juarez et al. 2014a) and Australia (Negron-Juarez et al. 2014b) and strong convective storms impacting Amazon forests (Negron-Juarez et al. 2010).

Estimating total tree mortality from Hurricane Maria, and how that mortality rate varies spatially across the island, will require new field investigations that will be carried out in 2018. An initial order-of-magnitude impact estimate based on remote sensing and field work carried out in landfalling hurricanes in U.S. forests (Negron-Juarez et al. 2014a) indicated that Hurricane

PeerJ Preprints | https://doi.org/10.7287/peerj.preprints.26597v1 | CC BY 4.0 Open Access | rec: 1 Mar 2018, publ: 1 Mar 2018

Maria may have caused mortality and severe damage to 23-31 million trees. Previous work has demonstrated that the relationship between ΔNPV and field measured mortality and damage rates is highly dependent on variability in forest stem density (Negron-Juarez et al. 2014b), and thus accurate maps of ΔNPV-derived mortality rates for different biogeographic regions depend on field measured mortality rates and stem density.

Acknowledgments
This research was supported by the Office of Science, Office of Biological and Environmental Research of the U.S. Department of Energy under Contract No. DE-AC02-05CH11231 as part of the Next-Generation Ecosystem Experiments–Tropics project and the Regional and Global Climate Modeling Program, and used resources of the National Energy Research Scientific Computing Center (NERSC), also supported by the Office of Science of the U.S. Department of Energy, under Contract No. DE-AC02-05CH11231.

PeerJ Preprints | https://doi.org/10.7287/peerj.preprints.26597v1 | CC BY 4.0 Open Access | rec: 1 Mar 2018, publ: 1 Mar 2018

Bibliography

Chambers, J. Q., J. I. Fisher, H. Zeng, E. L. Chapman, D. B. Baker, and G. C. Hurtt. "Hurricane Katrina's Carbon Footprint on U.S. Gulf Coast Forests." *Science* 318, no. 5853 (11, 2007): 1107. doi:10.1126/science.1148913.

Foster, D. R., M. Fluet, and E. R. Boose. "Human or Natural Disturbance: Landscape-Scale Dynamics of the Tropical Forests of Puerto Rico." *Ecological Applications* 9, no. 2 (05 1999): 555. doi:10.2307/2641144.

Friedl, Mark A., Damien Sulla-Menashe, Bin Tan, Annemarie Schneider, Navin Ramankutty, Adam Sibley, and Xiaoman Huang. "MODIS Collection 5 Global Land Cover: Algorithm Refinements and Characterization of New Datasets." *Remote Sensing of Environment* 114, no. 1 (01 2010): 168-82. doi:10.1016/j.rse.2009.08.016.

Frolking, S., M. W. Palace, D. B. Clark, J. Q. Chambers, H. H. Shugart, and G. C. Hurtt. "Forest Disturbance and Recovery: A General Review in the Context of Spaceborne Remote Sensing of Impacts on Aboveground Biomass and Canopy Structure." *Journal of Geophysical Research: Biogeosciences* 114, no. G2 (06 2009). doi:10.1029/2008jg000911.

Furby, S.l, and N.a Campbell. "Calibrating Images from Different Dates to 'like-value' Digital Counts." *Remote Sensing of Environment* 77, no. 2 (08 2001): 186-96. doi:10.1016/s0034-4257(01)00205-x.

Gorelick, Noel, Matt Hancher, Mike Dixon, Simon Ilyushchenko, David Thau, and Rebecca Moore. "Google Earth Engine: Planetary-scale Geospatial Analysis for Everyone." *Remote Sensing of Environment*, 07 2017. doi:10.1016/j.rse.2017.06.031.

Hansen, M. C., P. V. Potapov, R. Moore, M. Hancher, S. A. Turubanova, A. Tyukavina, D. Thau, S. V. Stehman, S. J. Goetz, T. R. Loveland, A. Kommareddy, A. Egorov, L. Chini, C. O. Justice, and J. R. G. Townshend. "High-Resolution Global Maps of 21st-Century Forest Cover Change." *Science* 342, no. 6160 (11, 2013): 850-53. doi:10.1126/science.1244693.

Hong, Yang, Robert Adler, and George Huffman. "Evaluation of the Potential of NASA Multi-satellite Precipitation Analysis in Global Landslide Hazard Assessment." *Geophysical Research Letters* 33, no. 22 (11, 2006). doi:10.1029/2006gl028010.

Huete, Alfredo R., Kamel Didan, Yosio E. Shimabukuro, Piyachat Ratana, Scott R. Saleska, Lucy R. Hutyra, Wenze Yang, Ramakrishna R. Nemani, and Ranga Myneni. "Amazon Rainforests Green-up with Sunlight in Dry Season." *Geophysical Research Letters* 33, no. 6 (2006). doi:10.1029/2005gl025583.

Justice, C.o., E. Vermote, J.r.g. Townshend, R. Defries, D.p. Roy, D.k. Hall, V.v. Salomonson, J.l. Privette, G. Riggs, A. Strahler, W. Lucht, R.b. Myneni, Y. Knyazikhin, S.w. Running, R.r. Nemani, Zhengming Wan, A.r. Huete, W. Van Leeuwen, R.e. Wolfe, L. Giglio, J. Muller, P. Lewis, and M.j. Barnsley. "The Moderate Resolution Imaging Spectroradiometer (MODIS): Land Remote Sensing for Global Change Research." *IEEE Transactions on Geoscience and Remote Sensing* 36, no. 4 (07 1998): 1228-249. doi:10.1109/36.701075.

Loveland, T. R., and A. S. Belward. "The IGBP-DIS Global 1km Land Cover Data Set, DISCover: First Results." *International Journal of Remote Sensing* 18, no. 15 (10 1997): 3289-295. doi:10.1080/014311697217099.

Negrón-Juárez, Robinson, David B. Baker, Hongcheng Zeng, Theryn K. Henkel, and Jeffrey Q. Chambers. "Assessing Hurricane-induced Tree Mortality in U.S. Gulf Coast Forest Ecosystems." *Journal of Geophysical Research* 115, no. G4 (12, 2010). doi:10.1029/2009jg001221.

Negrón-Juárez, Robinson, David B. Baker, Jeffrey Q. Chambers, George C. Hurtt, and Stephen Goosem. "Multi-scale Sensitivity of Landsat and MODIS to Forest Disturbance Associated

PeerJ Preprints | https://doi.org/10.7287/peerj.preprints.26597v1 | CC BY 4.0 Open Access | rec: 1 Mar 2018, publ: 1 Mar 2018

with Tropical Cyclones." *Remote Sensing of Environment* 140 (01 2014): 679-89. doi:10.1016/j.rse.2013.09.028.

Powell, Mark D., Sam H. Houston, Luis R. Amat, and Nirva Morisseau-Leroy. "The HRD Real-time Hurricane Wind Analysis System." *Journal of Wind Engineering and Industrial Aerodynamics* 77-78 (09 1998): 53-64. doi:10.1016/s0167-6105(98)00131-7.

Rifai, Sami W., José D. Urquiza Muñoz, Robinson I. Negrón-Juárez, Fredy R. Ramírez Arévalo, Rodil Tello-Espinoza, Mark C. Vanderwel, Jeremy W. Lichstein, Jeffrey Q. Chambers, and Stephanie A. Bohlman. "Landscape-scale Consequences of Differential Tree Mortality from Catastrophic Wind Disturbance in the Amazon." *Ecological Applications* 26, no. 7 (09, 2016): 2225-237. doi:10.1002/eap.1368.

Saha, Suranjana, Shrinivas Moorthi, Xingren Wu, Jiande Wang, Sudhir Nadiga, Patrick Tripp, David Behringer, Yu-Tai Hou, Hui-Ya Chuang, Mark Iredell, Michael Ek, Jesse Meng, Rongqian Yang, Malaquías Peña Mendez, Huug Van Den Dool, Qin Zhang, Wanqiu Wang, Mingyue Chen, and Emily Becker. "The NCEP Climate Forecast System Version 2." *Journal of Climate* 27, no. 6 (03 2014): 2185-208. doi:10.1175/jcli-d-12-00823.1.

Salomonson, V.v., D.l. Toll, and W.t. Lawrence. "Moderate Resolution Imaging Spectroradiometer [modis] And Observations Of The Land Surface." *[Proceedings] IGARSS '92 International Geoscience and Remote Sensing Symposium*. doi:10.1109/igarss.1992.576766.

Schwartz, Naomi B., María Uriarte, Ruth Defries, Kristopher M. Bedka, Katia Fernandes, Victor Gutiérrez-Vélez, and Miguel A. Pinedo-Vasquez. "Fragmentation Increases Wind Disturbance Impacts on Forest Structure and Carbon Stocks in a Western Amazonian Landscape." *Ecological Applications* 27, no. 6 (07, 2017): 1901-915. doi:10.1002/eap.1576.

Shutts, Glenn. "A Kinetic Energy Backscatter Algorithm for Use in Ensemble Prediction Systems." *Quarterly Journal of the Royal Meteorological Society* 131, no. 612 (10 2005): 3079-102. doi:10.1256/qj.04.106.

Skamarock, William C., and Joseph B. Klemp. "A Time-split Nonhydrostatic Atmospheric Model for Weather Research and Forecasting Applications." *Journal of Computational Physics* 227, no. 7 (03 2008): 3465-485. doi:10.1016/j.jcp.2007.01.037.

Walker, Lawrence R., Janice Voltzow, James D. Ackerman, Denny S. Fernandez, and Ned Fetcher. "Immediate Impact of Hurricane Hugo on a Puerto Rican Rain Forest." *Ecology* 73, no. 2 (04 1992): 691-94. doi:10.2307/1940775.

Zeng, H., J. Q. Chambers, R. I. Negron-Juarez, G. C. Hurtt, D. B. Baker, and M. D. Powell. "Impacts of Tropical Cyclones on U.S. Forest Tree Mortality and Carbon Flux from 1851 to 2000." *Proceedings of the National Academy of Sciences* 106, no. 19 (04, 2009): 7888-892. doi:10.1073/pnas.0808914106.

PeerJ Preprints | https://doi.org/10.7287/peerj.preprints.26597v1 | CC BY 4.0 Open Access | rec: 1 Mar 2018, publ: 1 Mar 2018